Modeling of the Mechanical Properties of a Wood-Fiber/Bicomponent-Fiber Composite

Herman van Dyk, Perry Peralta,* and Ilona Peszlen

An engineered composite that combines a wood fiber core, a bicomponent fiber face, and a bicomponent fiber back was evaluated for its elastic response using laminate theory. Using the properties of the individual laminae as input variables, the laminate's elastic modulus, axial strain, and lateral strain were determined by means of the model, and compared with values determined experimentally. The model yielded an axial elastic modulus of 950 MPa, which did not differ substantially from the measured value of 920 MPa. Statistical analyses showed that the measured and calculated strains were not significantly different in either the axial or lateral directions. The model underpredicted the strains along the fiber direction of the bicomponent fiber sheets by approximately 4%. A greater difference (12%) between predicted and measured values was observed in the lateral direction.

Keywords: Bicomponent fiber; Fiberboard; Needlepunching; Composite; Laminate; Elastic modulus; Shear modulus; Poisson's ratio

*Contact information: Department of Forest Biomaterials, North Carolina State University, Campus Box 8005, Raleigh, NC 27695 USA; *Corresponding author: perry_peralta@ncsu.edu*

INTRODUCTION

A composite in the engineering sense is any material that has been physically assembled from two or more materials to form one single bulk, but the resulting product would still have identifiable and distinct constituents within its structure. Composites are engineered to take advantage of the characteristics of each of the materials.

Usually, composite materials will consist of two separate components, the matrix and the filler. The matrix is the component that holds the filler together. It usually consists of various epoxy-type polymers, but other materials may be used. Metal matrix and thermoplastic matrix composites are some of the possibilities. The filler is the material that has been imbedded into the matrix to lend its advantage (usually strength) to the composite.

Composite materials have been widely utilized in the field of civil engineering, both in new constructions as well as in the reinforcement of existing concrete structures (Corradi *et al*. 2006). Most recently, these composites have also become popular in the forest products industry. Carbon and glass fiber reinforcement, in conjunction with an epoxy matrix, have been used for the reinforcement of wood and glulam beams (Triantafillou 1997; Triantafillou and Plevris 1991; Gentile *et al*. 2000). These types of reinforcement, called fiber-reinforced polymers (FRPs), are characterized by excellent mechanical properties, but the cost of both the fiber and the resin material can be prohibitive. Incompatible thickness swell characteristics also cause problems with regard to delamination (Lopez-Anido *et al*. 2005; Prian and Barkatt 1999).

There is currently no feasible method for efficiently reinforcing wood fiber products other than extruding the wood fiber with a polymer to form a wood plastic composite. Bicomponent fiber sheets offer the potential of reinforcing a wood fiber composite. Bicomponent fibers consist of at least two components, running parallel in the fiber throughout the length (Hutten 2007). Each of the components of the fiber retains its own characteristic properties. With sheath-core bicomponent fibers, the core component is completely surrounded by the sheath component. The sheath component has areas of interaction with the core and the surrounding medium. Commonly, the sheath polymer has a lower melting temperature than the core. During heating, the sheath will melt and diffuse through the surrounding fibers, acting as a binder (Bosak *et al*. 2005). Earlier work described one method of reinforcing a wood fiber panel by using polypropylene/polyester bicomponent fiber sheets in conjunction with needlepunching to form a sandwich laminate composite panel (van Dyk *et al.* 2009). The panel in question was manufactured by needlepunching a 1495 g/m^2 wood fiber web placed in between bicomponent fiber sheets. The panels were punched from both sides and then hot pressed for 3 min at 177 °C at a minimum pressure of 68 MPa. In order to fully understand the mechanical behavior of these panels, the elastic response of each of the laminae needs to be investigated, along with the response of the laminate.

This study will present a method for quantifying the engineering constants of the wood/bicomponent fiber composite developed by van Dyk *et al.* (2009), as well as the constants of each of the composite's constituent laminae. Furthermore, modeling of the behavior of the laminate formed with the different materials in question will be discussed.

Model to Predict Elastic Constants of a Lamina

If thickness strain is ignored, Hooke's law for plane stress in the 1,2–plane for orthotropic material may be written in terms of engineering constants as follows (Daniel and Ishai 2006):

$$\begin{bmatrix} \varepsilon_1 \\ \varepsilon_2 \\ \gamma_{12} \end{bmatrix} = \begin{bmatrix} \frac{1}{E_1} & -\frac{\nu_{12}}{E_1} & 0 \\ -\frac{\nu_{21}}{E_2} & \frac{1}{E_2} & 0 \\ 0 & 0 & \frac{1}{G_{12}} \end{bmatrix} \begin{bmatrix} \sigma_1 \\ \sigma_2 \\ \tau_{12} \end{bmatrix} \quad (1)$$

where σ_1 and σ_2 represent the axial stresses; τ_{12} is the shear stress; ε_1 and ε_2 are the axial strains; γ_{12} is the shear strain; ν_{12} and ν_{21} are the Poisson's ratios; E_1 and E_2 are the moduli of elasticity; and G_{12} is the shear modulus. It can be seen that four independent elastic constants are needed to characterize the material. The bicomponent layer of the laminate will be considered as an orthotropic material subjected to plane stresses. Based on the techniques used during the forming of the laminate panels, and data obtained for thickness swell studies, it was decided that the wood fiber core of the wood–bicomponent laminate panels was isotropic, and it was treated as such in the model. An isotropic material has three material constants (E, ν, and G), two of which are independent.

Macromechanical Model to Determine Elastic Behavior of a Laminate

The stresses in the different layers of a laminate can be expressed in terms of the laminate mid-plane strains and curvatures as follows (Daniel and Ishai 2006):

$$\begin{bmatrix} \sigma_x \\ \sigma_y \\ \tau_{xy} \end{bmatrix} = \begin{bmatrix} \overline{Q}_{11} & \overline{Q}_{12} & \overline{Q}_{16} \\ \overline{Q}_{12} & \overline{Q}_{22} & \overline{Q}_{26} \\ \overline{Q}_{16} & \overline{Q}_{26} & \overline{Q}_{66} \end{bmatrix} \begin{bmatrix} \varepsilon_x^o + z\kappa_x^o \\ \varepsilon_y^o + z\kappa_y^o \\ \gamma_{xy}^o + z\kappa_{xy}^o \end{bmatrix} \quad (2)$$

where,

ε_x^o = extensional strain of the reference surface (midplane) in the x direction

ε_y^o = extensional strain of the reference surface (midplane) in the y direction

γ_{xy}^o = inplane shear strain of the reference surface (midplane)

z = distance of a point from the midplane

κ_x^o = curvature of the reference surface (midplane) in the x direction

κ_y^o = curvature of the reference surface (midplane) in the y direction

κ_{xy}^o = twisting curvature of the reference surface (midplane)

$\left[\overline{Q}\right]$ = transformed reduced stiffness matrix

Equation 2 shows that the stresses vary linearly only through the thickness of each lamina. The stresses may change in magnitude from lamina to lamina because the transformed reduced stiffness matrix is dependent on the material and orientation of the ply. The stresses can be integrated in the thickness direction to yield the force resultants (N) and the moment resultants (M):

$$\begin{bmatrix} N_x \\ N_y \\ N_{xy} \end{bmatrix} = \int_{-h/2}^{h/2} \begin{bmatrix} \sigma_x \\ \sigma_y \\ \tau_{xy} \end{bmatrix} dz = \sum_{k=1}^{n} \int_{z_{k-1}}^{z_z} \begin{bmatrix} \sigma_x \\ \sigma_y \\ \tau_{xy} \end{bmatrix} dz \quad (3)$$

$$\begin{bmatrix} M_x \\ M_y \\ M_{xy} \end{bmatrix} = \int_{-h/2}^{h/2} \begin{bmatrix} \sigma_x \\ \sigma_y \\ \tau_{xy} \end{bmatrix} z\, dz = \sum_{k=1}^{n} \int_{z_{k-1}}^{z_z} \begin{bmatrix} \sigma_x \\ \sigma_y \\ \tau_{xy} \end{bmatrix} z\, dz \quad (4)$$

where,

n = number of layers

k = index for the ply number

h_k = thickness of each ply (where k=1 to n)

$h = \sum_{k=1}^{n} h_k$ = thickness of the laminate

z_i = z coordinate of each ply (where i=0 to n)

Layer 1 is bounded by z_0 and z_1

Layer k is bounded by z_{k-1} and z_k

Layer n is bounded by z_{n-1} and z_n

N = force per unit width of the laminate cross section

M = moment per unit width of the laminate cross section

Equations (2), (3), and (4) may be combined and then manipulated to give a single equation for calculating the strains and curvatures at the reference surface in terms of the force and moment resultants:

$$\begin{bmatrix} \varepsilon_x^o \\ \varepsilon_y^o \\ \gamma_{xy}^o \\ \kappa_x^o \\ \kappa_y^o \\ \kappa_{xy}^o \end{bmatrix} = \begin{bmatrix} A_{11} & A_{12} & A_{16} & B_{11} & B_{12} & B_{16} \\ A_{12} & A_{22} & A_{26} & B_{12} & B_{22} & B_{26} \\ A_{16} & A_{26} & A_{66} & B_{16} & B_{26} & B_{66} \\ B_{11} & B_{12} & B_{16} & D_{11} & D_{12} & D_{16} \\ B_{12} & B_{22} & B_{26} & D_{12} & D_{22} & D_{26} \\ B_{16} & B_{26} & B_{66} & D_{16} & D_{26} & D_{66} \end{bmatrix}^{-1} \begin{bmatrix} N_x \\ N_y \\ N_{xy} \\ M_x \\ M_y \\ M_{xy} \end{bmatrix} \quad (5)$$

where,

$$A_{ij} = \sum_{k=1}^{n} \left[\overline{Q}_{ij} \right]_k \left(z_k - z_{k-1} \right)$$

$$B_{ij} = \frac{1}{2} \sum_{k=1}^{n} \left[\overline{Q}_{ij} \right]_k \left(z_k^2 - z_{k-1}^2 \right)$$

$$D_{ij} = \frac{1}{3} \sum_{k=1}^{n} \left[\overline{Q}_{ij} \right]_k \left(z_k^3 - z_{k-1}^3 \right)$$

The [A] matrix, called the extensional stiffness matrix, relates the resultant in-plane forces to the in-plane strains. The [D] matrix, called the bending stiffness matrix, relates the resultant bending moments to the plate curvatures. The [B] matrix, called the bending-extension coupling stiffness matrix, couples the force and moment terms to the mid-plane curvatures and mid-plane strains. The 6 × 6 matrix consisting of the components of [A], [B], and [D] is called the laminate stiffness matrix or the *ABD* matrix.

EXPERIMENTAL

One method for measuring the elastic constants and the shear modulus needed for the model described in the previous section involves the use of two tensile test specimens, one with the primary material axis oriented along the longitudinal axis of a specimen and the second with the primary material axis oriented at 10 degrees to the longitudinal axis of the specimen (Chamis and Sinclair 1977). A T-rosette is installed on the on-axis specimen to measure the Poisson's ratio, while a three-element rectangular rosette is installed on the off- axis specimen (Fig. 1).

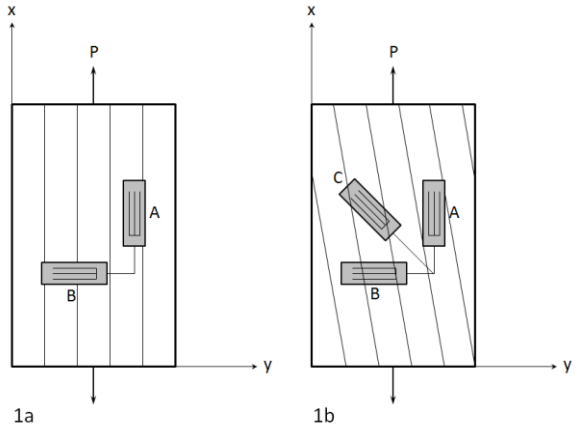

Fig. 1. Layout of the T-rosette (1a) and rectangular rosette (1b) strain gauge in the on-axis and 10-degree off-axis test specimens, respectively. P denotes the applied force. A, B, and C indicate the x, y, and 45° gages found on the rosettes, respectively.

The following describes strain gauge application techniques. Samples were prepared for the application of the strain gauge by lightly scuffing the surfaces with a high-grade sand paper. A placement grid was measured out on opposite faces to align the gauges. The gauges were placed face up in the center of a 25 mm by approximately 75 mm piece of clear adhesive tape to assist and maintain gauge alignment during gluing. Gauges were then held in place on the sample with the correct alignment by means of the tape, and partially lifted off prior to gluing leaving 35 mm of the tape in contact with the sample. An epoxy adhesive was prepared (Vishay M-Bond AE-10) in accordance with the supplier's specifications, and applied lightly to the surface of the gauge and the sample with a glass applicator. The adhesive tape was gently rolled down from the still-attached end by means of the applicator, squeezing out any excess resin. If done correctly, the gauge alignment is maintained through the entire process. A 25 mm by 25 mm silicon rubber pad was then placed on the gauge to evenly distribute the pressure, followed by a 25 mm by 25 mm block of wood. An 11-kg weight was placed on top of the entire assembly. The resin was left to dry overnight.

The Poisson's ratio, υ_{12}, can be calculated as follows from the strain measurements made with the T-rosette on the on-axis specimen:

$$\nu_{12} = \left| \frac{\varepsilon_B}{\varepsilon_A} \right| \quad (6)$$

where ε_A is the normal strain along the principal material axis which has the highest elastic modulus and ε_B is the strain along the material axis with the lowest elastic modulus. The remaining calculations are based on υ_{12} and the strain measurements obtained from the off-axis tensile test.

The strain gauge data obtained with the rectangular rosette shown in Fig. 1 can be used to calculate the shear strain, γ_{xy}, as:

$$\gamma_{xy} = \frac{\varepsilon_{45} - \varepsilon_x \cos^2 45 + \varepsilon_y \sin^2 45}{\sin 45 \cos 45} \tag{7}$$

where $\varepsilon_x = \varepsilon_A$, $\varepsilon_y = \varepsilon_B$, and $\varepsilon_{45} = \varepsilon_C$. Using standard strain transformations, the normal strains in the principal material axis (ε_1 and ε_2) and the shear strain (γ_{12}) can be calculated with:

$$\varepsilon_1 = \varepsilon_x \cos^2 \alpha + \varepsilon_y \sin^2 \alpha + \gamma_{xy} \sin \alpha \cos \alpha \tag{8}$$

$$\varepsilon_2 = \varepsilon_x \sin^2 \alpha + \varepsilon_y \cos^2 \alpha - \gamma_{xy} \sin \alpha \cos \alpha \tag{9}$$

$$\gamma_{12} = -2\varepsilon_x \sin \alpha \cos \alpha + 2\varepsilon_y \sin \alpha \cos \alpha + \gamma_{xy} \left(\cos^2 \alpha - \sin^2 \alpha \right) \tag{10}$$

where α is the counterclockwise rotation from the geometric axis to the material axis.

The normal stresses and shear stress for the principal material axis can be calculated with:

$$\sigma_1 = \frac{P \cos^2 \alpha}{bt} \tag{11}$$

$$\sigma_2 = \frac{P \sin^2 \alpha}{bt} \tag{12}$$

$$\tau_{12} = \frac{-P \sin \alpha \cos \alpha}{bt} \tag{13}$$

where P is the applied load, b is the specimen width, and t is the specimen thickness.

The elastic moduli, the shear modulus, and the remaining Poisson's ratio can then be calculated from:

$$E_1 = \frac{\sigma_1 - (\nu_{12} \sigma_2)}{\varepsilon_1} \tag{14}$$

$$E_2 = \frac{E_1 \sigma_2}{E_1 \varepsilon_2 + \sigma_1 \nu_{12}} \tag{15}$$

$$\nu_{21} = \nu_{12} \frac{E_2}{E_1} \tag{16}$$

$$G_{12} = \frac{\tau_{12}}{\gamma_{12}} \tag{17}$$

The experimental procedure was initially tested using radially sawn sassafras (*Sassafras albidum*) samples. The boards were selected according to straightness of grain. Sample beams with dimensions of 400 × 25 × 12.5 mm were cut with the grain aligned along the longitudinal axis of the beams for the on-axis tests. A T-rosette (Vishay 125LT) was adhered in the center of the 25-mm face, with a second linear strain gauge (Vishay 125LW) placed on the opposite face. For the 10-degree off-axis test, beams were cut from the boards by means of a tapering jig adjusted to 10 degrees. A triangular rosette gauge (Vishay 125LR) was used. Seven-mm holes were drilled in the ends of the beams. The stress was applied with a pin jig in an MTS testing machine. Strains were recorded with a Vishay Micro Measurements P3 Strain Indicator and Recorder. The resultant elastic moduli were compared with data obtained from the literature. In order to ascertain whether the gauge application was consistent, T and angular rosette gauges were applied to the same sample and the data obtained from the linear component of the gauges were compared. No significant differences were observed between the two results, which indicated that the gauge application technique worked adequately.

Wood–bicomponent fiber panels and medium-density fiberboard (MDF) were prepared according to the techniques described by van Dyk *et al*. (2009). It was decided to limit the tests conducted in this paper to the 2.3-mm panels due to the comparatively large differences observed in bending modulus between the 2.3-mm wood–bicomponent panels and the MDF control in the dynamic mechanical analysis. Furthermore, the sample dimensions were limited by the length of the panels produced to 200 mm × 18 mm × 2.3 mm. Samples were cut with a fiber orientation of the bicomponent sheets along the longitudinal axis of the beams, as well as at 10 degrees with respect to the beam axis.

To ensure that the stress distribution was even in the center of the beams where the gauges were placed, the ends were reinforced with an epoxy-reinforced paper sheet. The gauges were applied according to the procedure described previously. Samples were preloaded in the MTS testing machine at 2.5 mm/min until a load of 8.9 N was reached, after which the test proceeded at 1.25 mm/min. The tests were performed within the materials' linear elastic region, but in order to get good resolution the investigators followed the P3 Strain Indicator and Recorder manufacturer's recommendation to apply a large enough load to produce a longitudinal strain reading of at least 300 microstrains. The tests were stopped when a longitudinal strain reading of at least 600 microstrains was reached.

After conducting the tensile tests on the laminates, the bicomponent lamina was carefully removed from the surfaces by means of a paring knife. Care was taken to ensure that the gauges were not bent or otherwise damaged during removal. The delaminated bicomponent lamina was then retested in the MTS machine according to the procedure described above. Strain gauges were also attached to the delaminated wood fiber core after removal. The ends of these sections were also reinforced with the epoxy-infused paper sheets, and then tested in the MTS. A total of 15 bicomponent laminate panels were tested.

RESULTS AND DISCUSSION

For the delaminated wood fiber core, the stress-strain curve was used to calculate the modulus of elasticity (E), while the axial and lateral strain readings from the T-rosette

strain gage were used to determine the Poisson's ratio (ν). From the E and ν values, the shear modulus (G) was calculated using the following equation:

$$G = \frac{E}{2(1+\nu)} \tag{18}$$

The elastic moduli, Poisson's ratios, and shear moduli for the delaminated wood fiber cores are shown in Table 1. The core had a mean modulus of elasticity of 690 MPa (standard deviation 50 MPa), a mean Poisson's ratio of 0.29 (standard deviation 0.03), and a mean shear modulus of 270 MPa (standard deviation 20 MPa). Cai (2006) obtained values for the modulus of elasticity in tension for an MDF of 2000 MPa. This large discrepancy between the values obtained during this research and those cited in the literature can be attributed to the long press times used in this study to ensure that the bicomponent fiber surface reinforcement had adequate time at high temperature to melt the polypropylene sheath. Urea formaldehyde resin degrades when it is exposed to high temperature for long periods of time.

Table 1. Elastic Moduli, Poisson's Ratios, and Shear Moduli of Delaminated Wood Fiber Core (E, ν, and G) and of Delaminated Bicomponent Sheets (E_1, E_2, ν_{21}, and G_{12}) Obtained from Wood–Bicomponent Laminate Panels

Sample No.	Wood Fiber Core			Bicomponent Fiber Sheet			
	E (x10^9 Pa)	ν	G (x10^9 Pa)	E_1 (x10^9 Pa)	E_2 (x10^9 Pa)	ν_{12}	G_{12} (x10^9 Pa)
1	0.68	0.29	0.26	2.06	0.48	0.28	0.71
2	0.73	0.26	0.29				
4	0.70	0.21	0.29	2.24	0.64	0.28	0.85
5	0.60	0.28	0.24	2.38	0.72	0.29	0.53
6	0.66	0.30	0.25	2.05	0.34	0.28	0.63
7	0.73	0.30	0.28	2.20	0.35	0.32	0.70
8	0.73	0.33	0.27	2.21	0.53	0.28	0.87
9	0.66	0.29	0.25	2.10	0.42	0.28	0.82
10	0.68	0.30	0.26	2.27	0.58	0.30	0.84
11	0.70	0.30	0.27	2.17	0.49	0.28	0.68
12	0.78	0.29	0.30	2.05	0.38	0.30	0.77
14	0.69	0.29	0.27	2.20	0.42	0.28	0.77
15	0.63	0.30	0.24	2.38	0.72	0.29	0.53
Mean	0.69	0.29	0.27	2.19	0.51	0.29	0.73
St. Dev.	0.05	0.03	0.02	0.12	0.13	0.01	0.12

For the delaminated bicomponent fiber sheets, the Poisson's ratios (ν_{12}) were obtained from on-axis tensile tests; while the elastic moduli in the fiber direction (E_1), elastic moduli in the lateral direction (E_2), and the shear moduli (G_{12}) were obtained from the data produced by the off-axis tensile tests. Three samples were rejected after completion of the experiments. Bicosheet2 was rejected because the load cell reading from the testing machine did not register in the data acquisition system, Bicosheet3 was rejected after issues were observed with the strain gage adhesion to the wood fiber core, and Bicosheet13 was rejected due to one of the lead wires detaching during the testing procedure. A mean E_1 of 2200 MPa (standard deviation 120 MPa) and E_2 of 510 MPa (standard deviation 130 MPa) were observed. G_{12} and ν_{12} were 730 MPa (standard deviation 120 MPa) and 0.29 (standard deviation 0.01), respectively (Table 1).

The values listed in Table 1 for the delaminated bicomponent sheets and the corresponding values for the wood fiber core were used as inputs in the model described earlier for the whole laminate (Equation 5). By multiplying the inverse of the *ABD* matrix with the applied stress, the resultant strain at that stress level can be determined for the wood–bicomponent panels. These values were compared with the measured strain values obtained from on-axis tensile tests of the wood–bicomponent panels. In order to control for the time-dependent effect on the elastic properties of the material, it was decided to use stress and strain values taken at least 2 min after sample loading commenced in the MTS. Table 2 lists the experimentally measured ε_1 and ε_2, as well as values calculated from the model.

Table 2. Comparison of the Strains Measured During On-Axis Tensile Tests with the Calculated Strains for Each of the Wood–Bicomponent Panels Tested

Sample	Measured ε_1 (x 10^{-4})	Calculated ε_1 (x 10^{-4})	Measured ε_2 (x 10^{-4})	Calculated ε_2 (x 10^{-4})	% Deviation between Measured and Modeled Strains	
					ε_1	ε_2
bicopanel1	3.33	3.37	−0.96	−0.97	−1.1	−1.2
bicopanel2	3.35	3.21	−0.97	−0.84	4.3	13.0
bicopanel4	3.44	3.20	−1.02	−0.87	7.0	15.0
bicopanel5	3.33	3.02	−0.90	−0.83	9.3	8.3
bicopanel6	3.35	3.34	−0.99	−0.90	0.4	8.9
bicopanel8	3.35	3.19	−1.13	−0.87	4.7	23.4
bicopanel9	3.16	3.10	−0.98	−0.90	1.9	8.6
bicopanel10	3.33	3.52	−0.97	−1.06	−5.8	−8.9
bicopanel12	3.33	3.19	−1.08	−0.95	4.1	12.1
bicopanel14	3.37	3.30	−1.31	−1.01	2.0	22.7
bicopanel15	3.35	3.12	−1.01	−0.91	6.8	10.5
Mean	3.32	3.22	−1.03	−0.91	4.3	12.0
St. dev.	0.06	0.14	0.11	0.07	2.8	6.5

T-tests conducted to compare the means of the measured and calculated strains for the 1 and 2 directions showed no significant difference, indicating that the model previously discussed fit the experimental values well. It can be seen from Table 2 that the model underpredicts the strain in the bicomponent fiber direction by 4.3%. The model overpredicts the strains for bicopanel1 and bicopanel10. The underprediction can be attributed to interactions caused by the fibers passing through the thickness direction as a result of needlepunching not incorporated by the model.

In the direction lateral to the main orientation of the bicomponent fibers, a mean microstrain of −91 (standard deviation 7) was predicted by the model, while the measured microstrain was −103 (standard deviation 11). The model underpredicted the strain in the *y*-direction by 12.0% (standard deviation 6.5). The large deviation can be attributed to Bicopanel8 and Bicopanel14, both of which showed deviations from the measured values of greater than 20%. As was the case for the longitudinal strain, the model overpredicted the strains for Bicopanel1 and Bicopanel10.

The data in Table 1 were also used to calculate the effective elastic constants of the laminate. The model yielded a calculated elastic modulus of 950 MPa, which did not differ substantially from the measured value of 920 MPa. These results highlight the

benefit of incorporating a stiffer material in a laminate. Since the mean modulus of elasticity of the bicomponent fiber sheet along the fiber direction is almost three times the modulus of elasticity of the isotropic wood fiber core, it is to be expected that a bicomponent fiber sheet can serve as a reinforcing layer to a wood fiberboard. The calculated laminate property of 950 MPa represents a 38% improvement in the longitudinal elastic modulus over a fiberboard panel, even though the thickness of each of the bicomponent fiber sheets was only 9% of the panel thickness. Modeling of the effect of the bicomponent fiber sheet shows that increasing the thickness of each of the reinforcement layers further to 20% or 30% of the panel thickness will, respectively, result in 87% or 131% improvement in the composite panel modulus over a fiberboard panel. The Poisson's ratio of the bicomponent fiber sheet is about the same as the Poisson's ratio of the wood fiber core, thus the measured ratio of the laminate ($\nu_{12} = 0.30$) was close to the value predicted by the model ($\nu_{12} = 0.29$).

To further investigate the effects of the various parameters on the results obtained from the model, sensitivity analyses were conducted. Parameters investigated were the bicomponent fiber sheet moduli (E_1 and E_2), the wood fiber core modulus (E), and the wood fiber core Poisson's ratio (ν). The mean values obtained for each of the parameters were used as initial inputs in the model to calculate the longitudinal and lateral strains (ε_1 and ε_2). The parameters were then adapted according to the standard deviation approach employed by Skaggs and Bender (1995), who changed the input values by 2 standard deviation increments up to 6 standard deviations from the mean. The values calculated using this approach were then expressed as a percentage deviation from the values calculated using the mean inputs.

Figure 2 illustrates the variation from the mean when the parameter E_1, the longitudinal elastic modulus of the reinforcement, is changed. It can be seen that increasing the longitudinal stiffness by 2 standard deviations from the mean results in a 4% reduction in the calculated ε_1 and ε_2. The reduction is expected, seeing that an increase in elasticity will result in lower strains, if the stress is kept constant. The inverse occurs when the modulus is decreased by 2 standard deviations. When taken into account with the fact that model-calculated strains deviated from the measured strains by 4.3%, the importance of correctly identifying E_1 becomes apparent.

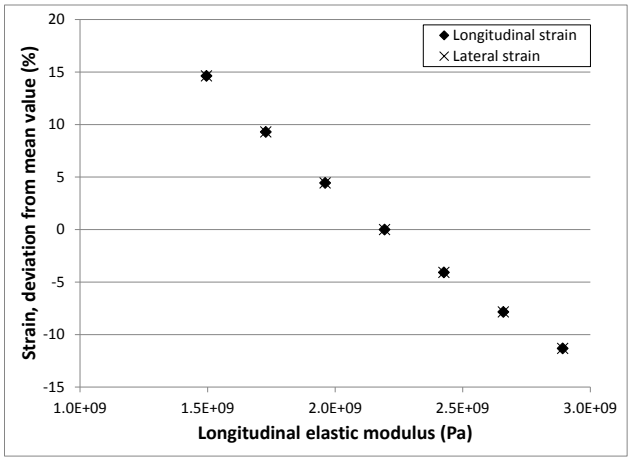

Fig. 2. Strains calculated with the macromechanical model by varying the mean longitudinal elasticity of the bicomponent fiber (E_1) by 2 standard deviation increments, expressed as a percentage of the values obtained using the mean elasticity

A ±6 standard deviation change in lateral stiffness E_2 of the bicomponent fiber sheets resulted in less than 0.05% change in the panel's longitudinal and lateral strains. The low sensitivity of the strains to variations in this input variable can be attributed to the closeness in the value of the mean E_2 of the bicomponent fiber sheet to the mean E of the wood fiber core, coupled with the low standard deviation of E_2.

As expected, an increase in the Poisson's ratio of the wood fiber core had a negligible effect on ε_1. It had, however, a strong effect on lateral strain ε_2. Increasing the Poisson's ratio of the wood fiber core even by just 2 standard deviations resulted in a 17% increase in panel lateral strain. A 6 standard deviation increase resulted in a whopping 51% increase in lateral strain. The effect of the elastic modulus E of the wood fiber core on calculated strains was less dramatic than that of the Poisson's ratio on ε_2 but nonetheless was significant. A 2 standard deviation decrease in E resulted in a 9% increase in ε_1 and ε_2; a 6 standard deviation decrease in E resulted in a 32% increase in ε_1 and ε_2. As expected, the model is highly sensitive to the properties of the wood fiber core, due to the fact that the core accounts for approximately 80% of the volume of the material. These results show that care needs to be taken in obtaining the properties of the core material when attempting to determine the tensile properties of the laminate.

To investigate the effect of needlepunching on the tensile properties of the material, an on-axis tensile test was conducted on a non-needlepunched wood fiberboard that was reinforced with bicomponent fiber sheets. The sample was prepared by thermally bonding the bicomponent fiber sheets to the surfaces of the wood fiberboard. Tensile tests were conducted as described previously. The modulus of elasticity of the non-needlepunched wood–bicomponent panel was 890 MPa. The mean modulus of elasticity obtained from on-axis tensile tests conducted on the needlepunched wood–bicomponent panels was found to be 920 MPa. The E of the non-needlepunched wood–bicomponent fiberboard was therefore slightly more than 1 standard deviation lower than that of the needlepunched wood–bicomponent panels. It is worth noting that the wood fiber core used for this particular experiment had an elastic modulus of 615 MPa, which is about 75 MPa less than the mean modulus of the needlepunched wood fiber core.

Further experiments were also conducted to verify the effectiveness of the model by adjusting the thickness of the bicomponent fiber reinforcement. These tests were conducted on non-needlepunched wood–bicomponent fiber panels. The panels were made with bicomponent fiber sheet thicknesses of 0.1, 0.2, 0.3, and 0.4 mm, after which they were prepared and tested by means of on-axis tensile tests. The measured strains were then compared with the calculated strains (Table 3). The means of the elastic constants for the bicomponent fiber sheets shown in Table 1 were used as inputs, while the constants for the non-needlepunched cores were obtained from on-axis tensile tests. It can be seen from the calculated strain values that the model is able to account for changes in the thickness of the reinforcement, with an increase in thickness resulting in a decrease in strain as the effective stiffness of the composite rises.

Table 3. Measured and Calculated Strains of Non-Needlepunched Wood–Bicomponent Fiber Panels with a Change in Thickness of the Bicomponent Fiber Reinforcement

Thickness of Reinforcement (mm)	Stress (Pa)	Measured ε_1 (x 10^{-4})	Calculated ε_1 (x 10^{-4})	Measured ε_2 (x 10^{-4})	Calculated ε_2 (x 10^{-4})	% Deviation between Measured and Modeled Strains	
						ε_1	ε_2
0.1	303590	3.8	4.1	−0.99	−1.2	6.19	15.1
0.2	305280	3.6	3.2	−0.89	−0.93	−11.1	4.51
0.3	303900	3.1	2.7	−0.71	−0.78	−14.9	8.56
0.4	307340	2.6	2.3	−0.54	−0.66	−12.5	18.8

CONCLUSIONS

1. A model for predicting the mechanical properties of a composite panel, which contains wood fiber in the core and a bicomponent fiber sheet used as surface reinforcement, was discussed. This model was successfully validated by means of experimental data obtained from tensile tests.
2. Sensitivity analyses were conducted to determine which parameters had the greatest effect on strains calculated by means of the model. It was found that lateral strains are especially sensitive to changes in lateral stiffness of the bicomponent fiber reinforcement, as well as the Poisson's ratio of the wood fiber core.
3. The model proved to be sensitive to changes in the thickness of the reinforcement, and the ability of the model to predict strains at different reinforcement thicknesses was experimentally verified.

REFERENCES CITED

Bosak, D. R., Ogale, A. A., and van Dun, J. (2005). "Bicomponent fibers derived from immiscible polymer blends," *Textile Research Journal* 75(1), 50-56.

Cai, Z. (2006). "Selected properties of MDF and flakeboard overlaid with fiberglass mats," *Forest Products Journal* 56(11/12), 142-146.

Chamis, C. C., and Sinclair, J. H. (1977). "10-deg off-axis test for shear properties in fiber composites," *Experimental Mechanics* 17(9), 339-346.

Corradi, M., Speranzini, E., Borri, A., and Vignoli, A. (2006). "In-plane shear reinforcement of wood beam floors with FRP," *Composites Part B: Engineering* 37(4-5), 310-319.

Daniel, I. M., and Ishai, O. (2006). *Engineering Mechanics of Composite Materials*, 2nd edition, Oxford University Press, New York.

Gentile, C., Svecova, D., Saltzberg, W., and Rizkalla, S. H. (2000). "Flexural strengthening of timber beams using GFRP," Proceedings, Third International Conference on Advanced Composite Materials in Bridge and Structures; Ottawa, Canada; August 15-18, 2000.

Hutten, I. M. (2007). *Handbook of Non-Woven Filter Media*, Elsevier Science & Technology, Oxford, UK.

Lopez-Anido, R. A., Muszynski, L., Gardner, D. J., Goodell, B., and Herzog, B. (2005). "Performance-based material evaluation of fiber-reinforced polymer-wood interfaces in reinforced glulam members," *Journal of Testing and Evaluation* 33(6), 385-394.

Prian, L., and Barkatt, A. (1999). "Degradation mechanism of fiber-reinforced plastics and its implications to prediction of long-term behavior," *Journal of Materials Science* 34(16), 3977-3989.

Skaggs, T. D., and Bender, D. A. (1995). "Shear deflection of composite beams," *Wood and Fiber Science* 27(3), 327-338.

Triantafillou, T. C. (1997). "Shear reinforcement of wood using FRP materials," *Journal of Materials in Civil Engineering* 9(2), 65-69.

Triantafillou, T. C., and Plevris, N. (1991) "Post-strengthening of R/C beams with epoxy bonded fiber composite materials," Proceedings, ASCE Specialty Conference on Advanced Composites Materials in Civil Engineering Structures, pp. 245-256.

van Dyk, H., Peralta, P., Peszlen, I., and Banks-Lee, P. (2009). "An innovative wood-fiber composite incorporating nonwoven textile technologies," *Forest Products Journal* 59(11/12), 11-17.

Article submitted: October 31, 2012; Peer review completed: February 10, 2013; Revised version accepted: May 23, 2013; Published: May 23, 2013.